Published in final edited form as:
Adv Mater. 2005 December 8; 18(2): 165–169. doi:10.1002/adma.200500438.

Three-Dimensional Microfluidic Tissue-Engineering Scaffolds Using a Flexible Biodegradable Polymer

Christopher J. Bettinger,
MEMS Technology Group, Charles Stark Draper Laboratory, 555 Technology Square, Cambridge, MA 02139 (USA)

Department of Materials Science and Engineering, Massachusetts Institute of Technology, 77 Massachusetts Avenue, Room E25-342, Cambridge, MA 02139 (USA)

Eli J. Weinberg,
MEMS Technology Group, Charles Stark Draper Laboratory, 555 Technology Square, Cambridge, MA 02139 (USA)

Department of Mechanical Engineering, Massachusetts Institute of Technology, 77 Massachusetts Avenue, Room E25-342, Cambridge, MA 02139 (USA)

Katherine M. Kulig,
Massachusetts General Hospital, Harvard Medical School, 55 Fruit Street, Boston, MA 02114 (USA)

Joseph P. Vacanti [Prof.],
Massachusetts General Hospital, Harvard Medical School, 55 Fruit Street, Boston, MA 02114 (USA)

Yadong Wang [Prof.],
Department of Biomedical Engineering, Georgia Institute of Technology, 313 Ferst Drive, BME 2113, Atlanta, GA 30332-0535 (USA)

Jeffrey T. Borenstein, and
MEMS Technology Group, Charles Stark Draper Laboratory, 555 Technology Square, Cambridge, MA 02139 (USA)

Robert Langer [Prof.]
Department of Chemical Engineering, Massachusetts Institute of Technology, 77 Massachusetts Avenue, Room E25-342, Cambridge, MA 02139 (USA), E-mail: rlanger@mit.edu

Organ loss and failure is one of the most critical issues facing the healthcare industry in developed nations. The shortage of available organ donors has driven the growth and expansion of the field of tissue engineering as a means of developing replacement tissues and organs[1, 2] including the liver.[3] Microfabrication and bio-microelectromechanical system (bio-MEMS) technology is an attractive tool for developing tissue-engineering systems because of the improved spatial resolutions over traditional scaffold fabrication techniques such as casting and porogen leaching,[4] gas foaming,[5] and three-dimensional printing.[6] Polymer scaffolds replica-molded on micromachined silicon substrates can achieve feature resolutions of less than 10 μm,[7] the same lengthscale of mammalian cells. Microfluidic bioreactors have been both fabricated and seeded with a variety of cell types, including endothelial cells[7–10] and hepatocytes.[10–12] However, one limiting factor in previous studies of microfluidic scaffolds has been the choice of material. Microfabricated silicon and replica-molded poly (dimethylsiloxane) (PDMS), although ubiquitous and inexpensive, are not biodegradable and have limited biocompatibility, and therefore are not suitable biomaterials for a tissue-engineering scaffold. Microfluidic scaffolds fabricated from poly(L-lactic-*co*-glycolic acid) (PLGA),[13] while biodegradable, exhibit suboptimal properties for an implant material, such as rigid mechanical properties,[14] undesirable bulk degradation kinetics,[15] and limited

biocompatibility in some cases.[16] High concentrations of PLGA byproducts has also been shown to be cytotoxic,[17] which is a major limitation in the prospect of fabricating large, organ-size scaffolds.

Poly(glycerol sebacate) (PGS), a recently synthesized bio-compatible and biodegradable elastomer with superior mechanical properties, serves as a promising alternative material for fabricating microfluidic vascular scaffolds,[15] nerve guides,[18] as well as other microscale tissue-engineering systems. PGS is a tough, biodegradable elastomer that is biocompatible, inexpensive, and easy to synthesize from glycerol and sebacic acid. Glycerol and polymers containing sebacic acid have already been approved for use in medical applications. Biocompatibility studies[15,16] suggest improved cellular response and morphology of PGS compared to PLGA. PGS is also a suitable material for microfluidic scaffolds from a processing perspective. PGS prepolymer can be replica molded and cured on silicon masters to form layers as thin as 100 μm in a process that is analogous to replica molding of PDMS.[19]

Controlling the cellular microenvironment within scaffolds is critical for eliciting desirable biological responses such as proliferation, migration, and maturation. Maintaining suitable oxygen concentrations is of paramount importance in the culture of highly metabolic cells, such as hepatocytes, in microfluidic devices.[20] Therefore, elucidating the relevant transport properties of oxygen and carbon dioxide in PGS is essential in the determination of gas concentrations in the cell microenvironment. The mechanical microenvironment has also been shown to be critical in cellular function[21] in various cell types including endothelial cells.[22,23] Fluid shear stresses imposed on cells within microfluidic devices can lead to detachment and death. Therefore, it is important to consider the effect of shear stress that cells might experience within the microfluidic scaffold. In this work, we have developed microfabrication and replica-molding techniques specific to PGS. Single-layer microfluidic networks designed to promote hepatocyte adhesion and proliferation were stacked and bonded to create three-dimensional scaffold networks with high spatial densities of microchannels. Chemical and mechanical aspects of the cellular microenvironment were predicted using known device and material properties, and suitable operating conditions were implemented using this information. These net works were seeded with hepatocytes, which grew to form confluent layers in perfusion culture using adequate microenvironment parameters.

Scheme 1 illustrates the process flow for microfabrication of multilayered PGS devices. Scanning electron microscopy (SEM) images supported by rhodamine flow experiments verified the patency of the device (Figs. 1D–F). It is hypothesized that the ability for PGS layers to bond via covalent cross-linking has resulted in high-strength interfaces between PGS layers, which are virtually indistinguishable in the SEM cross-section of a typical microchannel (Fig. 1D). Devices containing up to five microfluidic layers were stacked and bonded; however, cell-culture experiments were performed in devices with two layers. The microchannels have a trapezoidal cross-sectional geometry instead of the expected rectangular shape. The presence of “feet” can be attributed to a sucrose accumulation artifact after baking the sacrificial sucrose layer. Knowledge of the relevant transport coefficients of oxygen and carbon dioxide in PGS is critical when designing complex, multilevel tissue-engineering systems (Table 1). Using this knowledge, it is possible to determine the critical lengthscale for mass transport within PGS for designing solid supports with substantial volumes for tissue-engineering applications. To study the lengthscale of diffusion limits of solid PGS, a simple mass-transfer problem[24] involving the supply of oxygen via diffusion across a layer of PGS to a monolayer of mammalian cells[25] was studied. This calculation suggests that PGS membranes have a maximum allowable thickness of approximately 232 μm to avoid hypoxic oxygen concentrations (≤1%).[26] To promote proliferation and other highly metabolic cellular activities, it is desirable to maintain an adequately oxygenated microenvironment. Therefore, it is valid to assume that the diffusion component of the oxygen supply is negligible, and

consequently the oxygen for the cells within the device will be supplied via the media. To this end, ensuring a well-oxygenated environment requires frequent reactor volume exchange, hyperoxygenated media, or both to achieve sufficient concentrations within the media to supply the entire cell population within the device.

Two device layouts, termed vascular and hepatocyte constructs (Fig. 1A), were designed and fabricated. The vascular construct has the unique property of exhibiting constant maximum shear stress within each channel of the device, making it a promising construct for an artificial vasculature tissue engineering scaffold.[27] The general layout of the hepatocyte design was designed to allow for high perfusion rates while also maximizing cell attachment. Therefore, a network of staggered posts was used to protect the cells from shear forces associated with high perfusion rates. The posts were flanked on either side by direct microchannels to reduce pressures within the device during operation at high volumetric flow rates. Finite-element fluid-dynamics simulations predicted extremely high flow rates along the microchannels that flank the network of posts. Two-layer microfluidic PGS devices featuring the hepatocyte construct (Fig. 2A) were statically seeded with hepatocyte carcinoma cells (HepG2, Figs. 2B,C), which were used as a model for human hepatocytes.[28,29] Due to the extremely high cell densities used in the initial seeding, cellular attachment occurred in virtually all microchannels throughout the device within hours. The high cell-seeding density resulted in the formation of HepG2 aggregates, which increased the opportunity for adhesion of cells to the microstructures. Long-term cell viability was inferred from cellular attachment within the microchannels.[30] Albumin production was also measured every 24 h to assess the liver-specific cell function of the seeded cells.[31] The albumin production rate was measured to be 24.3±5.5 μg cm^{-2} day^{-1}, which was comparable with previous reports.[10,12] A maximum albumin production rate of 30.5±0.2 μg day^{-1} per device occurred during the first 24 h, which can be attributed to the albumin production of cells located in the waste container that did not attach during the seeding. Reactors were perfused for a period of up to one week to demonstrate long-term viability within the devices.

The fabrication process described in this work is fast, efficient, and scalable. One key advantage to this technique is the ability for the polymer to be cured and bonded without the use of additional cytotoxic solvents or adhesives. The ability to segregate flow in multilayered devices makes these scaffolds suitable for incorporating multiple cell types within the three-dimensional scaffold (Fig. 2F). We feel this aspect of device functionality is a critical development in the design and fabrication of tissue-engineering scaffolds for highly vascularized tissue. These biodegradable microfluidic systems can also be integrated with existing biomaterial systems and technologies for tissue-specific applications and increased functionality. For example, drug-delivery systems,[32] cell-patterning techniques,[33,34] contact guidance cues,[35] and co-culture systems for hepatocytes[36] can be integrated within the micro-channels to promote the organization of primitive seeded cells into complex tissues. Fully biodegradable systems suitable for implantation can be fabricated by integrating flexible, small-caliber PGS tubes and affixing those using PGS prepolymer as an adhesive (data not shown). The end result is an adaptable tissue-engineering device that can be easy integrated with the patient's existing vasculature.

Experimental

PGS Membrane Synthesis

PGS prepolymer [15] was cured into flat sheets approximately 1 mm in thickness for 15 h at 150 °C at 50 mtorr (1 mtorr ~ 133 mPa). The membrane was placed in an aluminum machined diffusion chamber and evacuated for at least 120 h by applying vacuum to both sides across the membrane. After the evacuation procedure, the sample gas was supplied at a pressure of 1 atm (1 atm ~ 101.3 kPa) to the top side of the membrane, and the pressure was continuously

measured and recorded on the bottom side using a digital pressure transducer (MKS Instruments, Wilmington, MA) and LabVIEW software. Each experiment produced a time evolution of pressure, which was used to calculate the solubility, diffusivity, and permeability [37].

Computational Fluid Dynamics

Flow modeling was performed using the FEMLAB 3.0a finite-element simulation software (COMSOL Inc., Los Angeles, CA). A two-dimensional model for incompressible flow was used to determine the flow rates throughout the reactor using device-symmetry arguments. Appropriate boundary conditions were imposed consisting of a volumetric flow rate at the inlet, a neutral condition at the outlet, and a combination of slip and no-slip boundary conditions throughout the interior boundaries of the model geometry.

Device Design and Fabrication

Microfluidic networks were simulated using a finite-element simulation. The finalized mask layouts were converted to DXF files using AutoCAD 2000 and printed onto 1/20 mil (1 mil = 2.54×10^{-2} mm) transparencies (International Phototool, Colorado Springs, CO). Standard photolithographic and plasma-etching techniques were utilized to produce “negative mold” silicon masters for use in replica molding, just as PDMS can be used to fabricate microfluidic devices quickly and easily [19]. Briefly, patterns printed on high-resolution transparency films were transferred to chrome-on-glass masks to be used in the photolithography step. 100 mm diameter wafers were patterned with photoresist using one photolithography cycle. Features were etched using an STS etcher (Surface Technology Systems, Newport, UK) using etch-passivation cycles to yield a constant feature height of 50±2 μm across the wafer. The remaining photoresist was stripped in a series of acetone, isopropanol, and methanol rinses. Prior to replica molding of PGS, a sacrificial sucrose release layer was spin-coated on the silicon master. Micromachined silicon masters were cleaned using piranha solution (Mallinckrodt, St. Louis, MO) and plasma-cleaned (March, St. Petersburg, FL) at 250 mtorr and 200 W for 180 s. A 90% (w/w) solution of sucrose (Sigma, St. Louis, MO) in water was spin-coated at 3000 revolutions per minute for 30 s. The sucrose layer was pre-baked on a hot plate at 95 °C for 120 s and post-baked in an oven at 120 °C for 24 h. 1.7±0.05 g of PGS prepolymer was melted at 160 °C and applied to the wafers for replica molding and smooth sheet formation. The thickness of the final PGS film could be adjusted simply by varying the mass of prepolymer used. The prepolymer was cured at temperatures ranging from 135 to 140 °C for 18 h under 50 mtorr of vacuum, which produced a crosslinked sheet in which a portion of the hydroxyl and carboxylic acid functional groups remained. The PGS sheets were delaminated by statically incubating the polymer-master system in doubly distilled water (ddH_2O) at 24°C for 24 h beginning immediately after polymer curing. Diffusion of water between the polymer/silicon interface led to sucrose dissolution and eventual delamination. The sheets were trimmed and punched to achieve appropriate fluidic connections between layers. The microfluidic layers were stacked, aligned at 24 °C, and bonded together simultaneously by curing the polymer at 120 °C for 15 h under 50 mtorr of vacuum. Once the final curing step was completed, silicone tubing (1/16 in. inner diameter, 1/8 in. outer diameter (1 in.= 2.54 cm), Cole-Parmer) was inserted into the devices in a sterile environment. Luer-Lok connections were inserted into the tubing, and the base of the connections was sealed with epoxy (McMaster-Carr). In some cases, additional PDMS structures were added to the inlet and outlet to prevent dissociation of the tubing from the device. Samples used for SEM were sputter-coated with gold/palladium using a Cressington 108 Auto sputter coater (Cressington Scientific Instruments Inc., Valencia, PA). Scanning electron microscopy images were taken using a Hitachi S-3500N at 5 kV. Fluorescent micrographs were obtained by flowing 100 μm mL^{-1} rhodamine and 100 μm mL^{-1} 4,6-diamidino-2-phenylindole (DAPI) solutions in phosphate-buffered saline (PBS, Sigma, St. Louis, MO).

Cell Culture

All cell-culture products were obtained from Invitrogen Inc. (Carlsbad, CA) unless otherwise noted. Hepatocyte carcinoma cells (HepG2, ATCC, Manassas, VA) were cultured with Eagle's Modified Essential Medium supplemented with 10 % fetal bovine serum, 25 mM *N*-(2-hydroxylethyl)piperazine-*N*′-(2-ethanesulfonic acid) (HEPES), 100 μm mL^{-1} streptomycin, and 100 U mL^{-1} penicillin, at 37 °C and 5 % CO_2. Cells were harvested using Trypsin 0.025 %/ethylenediaminetetraacetic acid (EDTA) 0.01 % and quenched with an equal volume of medium to resuspend the cells. PGS devices were prepared for seeding by incubating with medium for 24 h and with 0.1 % collagen solution (Sigma, St. Louis, MO) for 2h at 37 °C immediately prior to cell seeding. The devices were statically seeded for 2 h to allow for cell attachment using cellular concentrations of approximately 5×10^8 cells mL^{-1}. After this period, the devices were set up in a linear perfusion circuit consisting of a syringe pump (New Era Pump System NE-1600, Farmingdale, NY), media reservoir, microfluidic scaffold, and media waste container. Fresh medium was perfused in a non-pulsatile manner with a volumetric flow rate of 280 μmh^{-1} to feed a two-layer device. Albumin samples were taken every 24h by sampling the waste container and aspirating the remaining medium to ensure the accuracy of future sampling. Upon stoppage of perfusion, cells were fixed by manually injecting the device with 3.7 % (v/v) paraformaldehyde in PBS (Sigma, St. Louis, MO) with a syringe under high hydrostatic pressure. This simultaneously fixed the cells and induced swelling and delamination of the PGS sheets. The sheets were sectioned and serially immersed in solutions of 25 %, 50 %, 75 %, and 90 % (v/v) ethanol in doubly distilled H_2O for 5 min each. The samples were then immersed in 100 % ethanol followed by hexamethyldisilazane (HMDS, Sigma, St. Louis, MO) each for 15 min. The samples were then allowed to air-dry for 24 h prior to imaging. Optical imaging was performed using a Carl Zeiss inverted microscope with AxioCam software. Albumin production was determined by a human enzyme-linked immunosorbent assay (ELISA) quantification kit (Bethyl Laboratories, Montgomery, TX) with absorption measurements made at 450 nm using a SpectraMax Plus 384 plate reader (Molecular Devices, Sunnyvale, CA) equipped with SOFTmax Pro 4.0 software.

Acknowledgments

The authors acknowledge the following: The MEMS Technology Group at the Draper Laboratory for direct funding and use of facilities; Kevin King, Brian Orrick, Mert Prince, Connie Cardoso, and Ashish Misra for their contributions in microfabrication and cell cul ture; and Mohammad Kaazempur-Mofrad for his assistance in the design and simulation of the constant shear networks. This work was supported by the National Institutes of Health (Grants HL 060435 and DE 013023). The views expressed are not endorsed by the sponsor. Additional funding provided by DL-H-550154. The content of this paper does not necessarily reflect the position or the policy of the government, and no official endorsement should be in ferred. Supporting Information is available online from Wiley Inter-Science or from the author.

References

1. Langer R, Vacanti JP. Science 1993;260:920. [PubMed: 8493529]
2. Griffith LG, Naughton G. Science 2002;295:1009. [PubMed: 11834815]
3. Kulig KM, Vacanti JP. Transplant Immunol 2004;12:303.
4. Murphy WL, Dennis RG, Kileny JL, Mooney DJ. Tissue Eng 2002;8:43. [PubMed: 11886653]
5. Harris LD, Kim BS, Mooney DJ. J. Biomed. Mater. Res 1998;42:396. [PubMed: 9788501]
6. Giordano RA, Wu BM, Borland SW, Griffith-Cima L, Sachs EM, Cima MJ. J. Biomater. Sci., Polym. Ed 1996;8:63. [PubMed: 8933291]
7. Borenstein JT, Terai H, King KR, Weinberg EJ, Kaazempur-Mofrad MR, Vacanti JP. Biomed. Microdevices 2002;4:167.
8. Kaihara S, Borenstein JT, Koka R, Lalan S, Ochoa ER, Ravens M, Pien H, Cunningham B, Vacanti JP. Tissue Eng 2000;6:105. [PubMed: 10941206]

9. Fidkowski C, Kaazempur-Mofrad MR, Borenstein JT, Vacanti JP, Langer R, Wang Y. Tissue Eng 2005;11:302. [PubMed: 15738683]
10. Leclerc E, Yasuyuki S, Fujii T. Biomed. Microdevices 2003;5:109.
11. Powers MJ, Domansky K, Kaazempur-Mofrad MR, Kalezi A, Capitano A, Upadhyaya A, Kurzawski P, Wack KE, Stolz DB, Kamm R, Griffith LG. Biotechnol. Bioeng 2002;78:257. [PubMed: 11920442]
12. Leclerc E, Sakai Y, Fujii T. Biotechnol. Prog 2004;20:750. [PubMed: 15176878]
13. King KR, Wang CCJ, Kaazempur-Mofrad MR, Vacanti JP, Borenstein JT. Adv. Mater 2004;16:2007.
14. Leatrese DH, Kim BS, Mooney DJ. J. Biomed. Mater. Res 1998;42:396. [PubMed: 9788501]
15. Wang Y, Ameer GA, Sheppard BJ, Langer R. Nat. Biotechnol 2002;20:602. [PubMed: 12042865]
16. Wang Y, Kim YM, Langer R. J. Biomed. Mater. Res., Part A 2003;66:192.
17. Ignatius AA, Claes LE. Biomaterials 1996;17:831. [PubMed: 8730968]
18. Sundback CA, Shyu JY, Wang Y, Faquin WC, Langer RS, Vacanti JP, Hadlock TA. Biomaterials 2005;26:5454. [PubMed: 15860202]
19. Duffy DC, McDonald JC, Schueller JA, Whitesides GM. Anal. Chem 1998;70:4974.
20. Clementi E, Brown GC, Foxwell N, Moncada S. Proc. Natl. Acad. Sci. USA 1999;96:1559. [PubMed: 9990063]
21. Resnick N, Yahav H, Shay-Salit A, Shushy M, Schubert S, Zilberman L, Wofovitz E. Prog. Biophys. Mol. Biol 2003;81:177. [PubMed: 12732261]
22. Dewey CF, Bussolari SR, Gimbrone MA, Davies PF. J. Biomech. Eng 1981;103:177. [PubMed: 7278196]
23. Malek AM, Izumo S. Am. J. Physiol 1992;263:C389. [PubMed: 1514586]
24. Incropera, FP.; Dewitt, DP. Fundamentals of Heat and Mass Transfer. New York: Wiley; 2002.
25. Clementi EG, Brown GC, Foxwell N, Moncada S. Proc. Natl. Acad. Sci. USA 1999;96:1559. [PubMed: 9990063]
26. Collard CD, Agah A, Stahl GL. Immunopharmacology 1998;39:39. [PubMed: 9667422]
27. Weinberg EJ, Borenstein JT, Kaazempur-Mofrad MR, Orrick B, Vacanti JP. Mater. Res. Soc. Symp. Proc 2004;820:121.
28. Aden DP, Fogel A, Potkin S, Damjanov I, Knowles BB. Nature 1979;282:615. [PubMed: 233137]
29. Kelly JH. US Patent 1994;5:290–684.
30. Re F, Zanetti A, Sironi M, Polentarutti N, Lanfrancone L, Dejana E, Colotta F. J. Cell Biol 1994;127:537. [PubMed: 7523422]
31. Cereghini S, Blumenfeld M, Yaniv M. Genes Dev 1988;2:957. [PubMed: 3169549]
32. Richardson DM, Peters MC, Ennet AB, Mooney DJ. Nat. Biotechnol 2001;19:1029. [PubMed: 11689847]
33. Suh KY, Seong J, Khademhosseini A, Laibinis PE, Langer R. Biomaterials 2001;25:557. [PubMed: 14585705]
34. Khademhosseini A, Suh KY, Yang JM, Eng G, Yeh J, Leven-berg S, Langer R. Biomaterials 2004;25:3583. [PubMed: 15020132]
35. Flemming RF, Murphy CJ, Abrams GA, Goodman SL, Nealey PF. Biomaterials 1999;20:573. [PubMed: 10213360]
36. Bhatia SN, Balis UJ, Yarmush ML, Toner M. FASEB J 1999;13:1883. [PubMed: 10544172]
37. Sok, RM. Ph.D. Thesis. The Netherlands: University of Groningen; 1994.

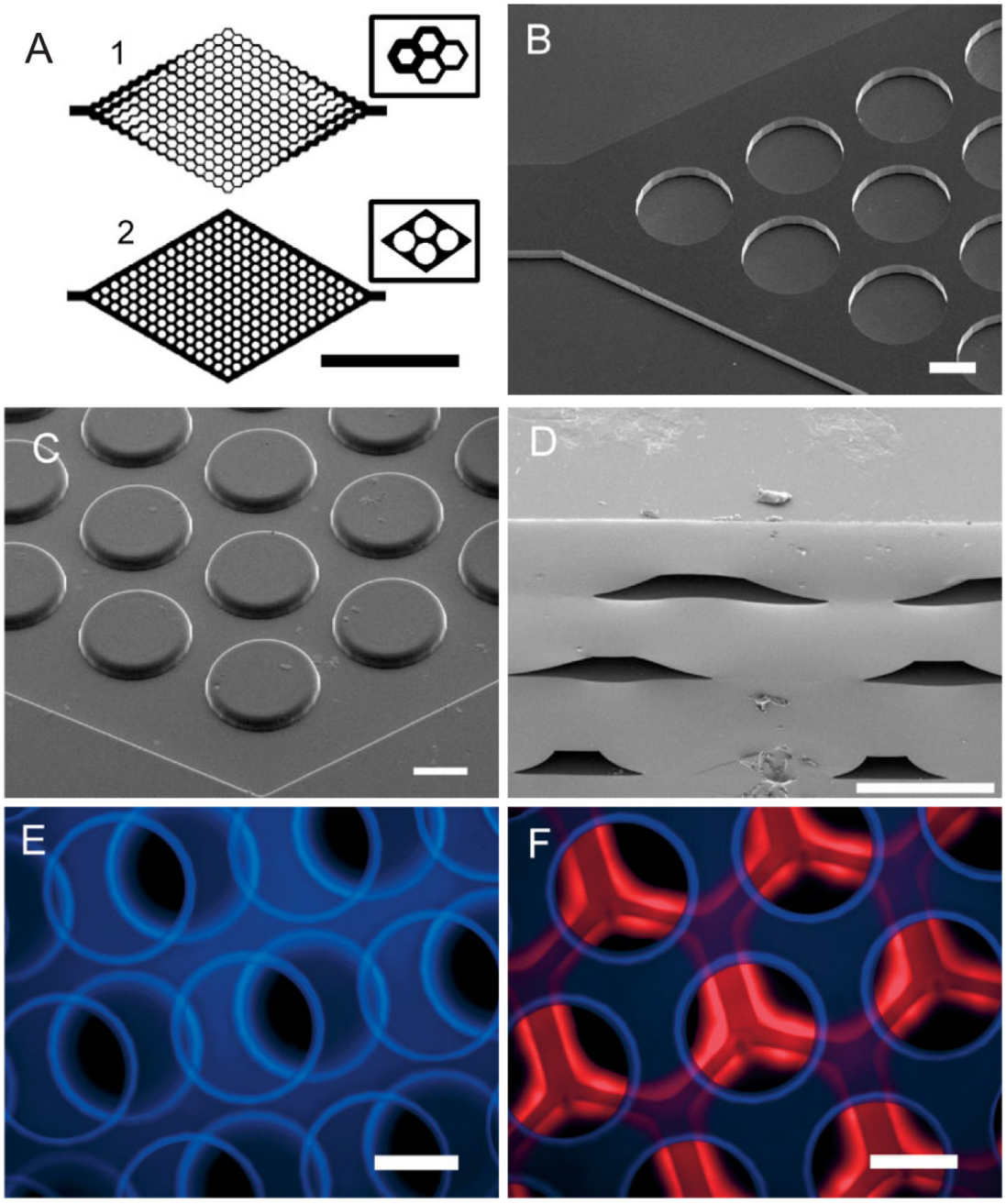

Figure 1.

Characterization of PGS microfluidic devices. A) Mask layout for vascular (1) and hepatocyte (2) networks were designed and fabricated using AutoCAD 2000 (Inlet ports are omitted to show detail; scale bar is 5 mm). Insets show detailed schematics of the representative microstructures used in each two-dimensional layout. B) SEM of micro-machined silicon "negative" masters designed for polymer replica molding of microfluidic hepatocyte networks. C) Replica-molded PGS layer of silicon master in (B). The rounded features are a result of an accumulation effect of sucrose (see Scheme 1). D) SEM cross-sections of three-layer PGS device. E,F) Composite fluorescent micrographs of devices after flowing rhodamine and 4,6-

diamidino-2-phenylindole (DAPI) solutions to demonstrate the patency of multilayer hepatocyte devices. (Scale bars in B–F are all 200 μm).

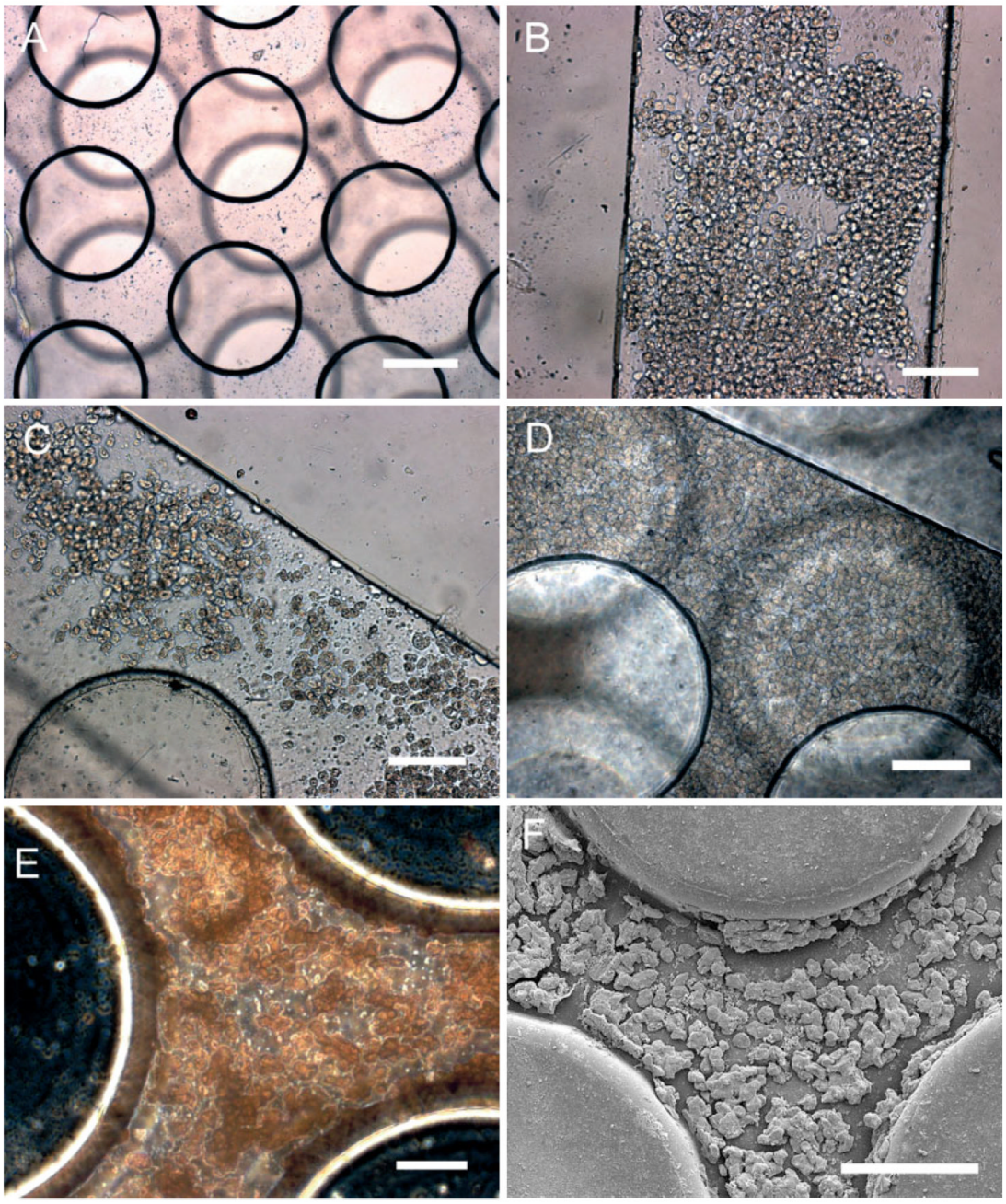

Figure 2.
Seeding and long-term culture of hepatocytes in microfluidic scaffolds. A) Bright-field optical micrograph of three-dimensional PGS device prior to cell seeding (scale bar is 200 μm). Immediately after seeding, partially confluent layers of cells are demonstrated B) at the inlet and C) in the post network. After 24 h, cell layers become confluent throughout the device (Scale bars in B–D are 200 μm). Devices were perfused for more than one week, and albumin production was measured to assess liver-specific cell function (see text). Upon stoppage of perfusion, cells were fixed and the devices were sectioned and imaged E) optically and F) using SEM (scale bars in (E) and (F) are 50 and 100 μm, respectively).

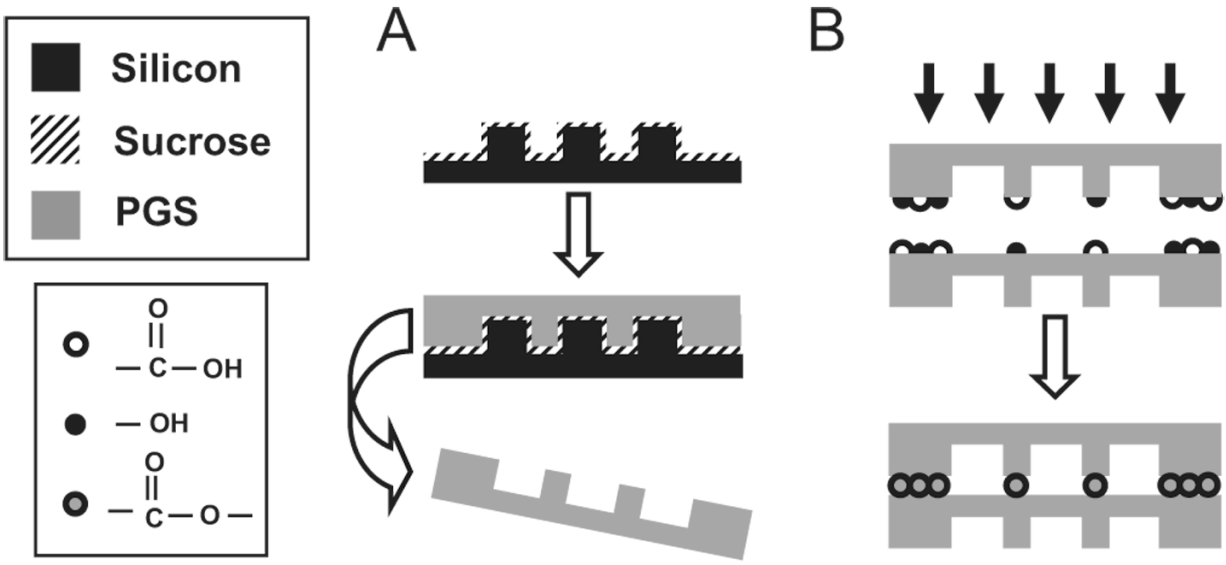

Scheme 1.
Overview of fabrication strategy for PGS microfluidic devices. A) Replica molding of PGS layers. Silicon substrates are micromachined and spin-coated with sucrose to serve as a sacrificial release layer (not shown). PGS prepolymer is cured into micropatterned sheets and delaminated in water. B) Multiple layers are bonded by physically adhering individual sheets and curing the films together. It is hypothesized that the additional curing step forms ester linkages from active hydroxyl and acid groups between layers.

Table 1

Permeabilities, diffusivities, and solubilities of oxygen and carbon dioxide in solid PGS at 24 °C.

Transport parameter	Oxygen (n = 7) [a]	Carbon dioxide (n = 7) [a]
Permeability (P) [Barrers] [b]	8.31 (± 1.05)	18.1 (± 4.58)
Diffusivity (D) [10^{-8} cm^2 sec^{-1}]	3.42 (± 1.17)	2.15 (± 0.49)
Solubility (S) [cm^3 gas (STP) cm^{-3} polymer atm^{-1}]	1.84 (± 0.79)	6.41 (± 0.26)

[a] Standard deviations are given in parentheses.

[b] 1 Barrer= 10^{-10} cm^3 gas (at STP) cm^{-2} s^{-10} cm Hg^{-1}.